Journal of Power Sources 256 (2014) 424–429

Contents lists available at ScienceDirect

Journal of Power Sources

journal homepage: www.elsevier.com/locate/jpowsour

Short communication

# A rapid preparation of acicular Ni impregnated anode with enhanced conductivity and operational stability

Xingbao Zhu [a,*], Chengzhi Guan [a,b,*], Zhe Lü [a], Bo Wei [a], Yiqian Li [a], Wenhui Su [a]

[a] Department of Physics, Harbin Institute of Technology, Heilongjiang 150080, People's Republic of China
[b] Center for Thorium Molten Salt Reactor System, Shanghai Institute of Applied Physics, Shanghai 201800, People's Republic of China

## HIGHLIGHTS

- A novel method is proposed to prepare Ni impregnated YSZ anode.
- A novel needle-shaped Ni is presented after a drying and heating process.
- The preparation efficiency for Ni impregnated YSZ anode is improved by 3 times.
- The specific surface area of anode is improved by 1.14 times.
- The conductivity and operational stability of the anode are improved substantially.

## ARTICLE INFO

*Article history:*
Received 4 October 2013
Received in revised form
11 January 2014
Accepted 16 January 2014
Available online 23 January 2014

*Keywords:*
Solid oxide fuel cell
Nano-anode
Microstructure
Infiltration
Needle-shaped
Vacuum drying

## ABSTRACT

A novel method for fabricating $Ni(NO_3)_2$ solution impregnated YSZ (YSZ: Yttria Stabilized Zirconia) anodes for solid oxide fuel cells (SOFCs) is presented. In order to reduce the impregnation cycles and increase the reliability of the YSZ membrane, a YSZ support with a porosity of ~60% is soaked in a saturated $Ni(NO_3)_2$ solution with an increased temperature of 80 °C. The impregnated anode is dried in a vacuum drying device without heating, resulting in a flower-like $Ni(NO_3)_2 \cdot 6H_2O$ crystal. The formed porous structure is likely to facilitate the impregnating process and considered to be the key to success of the impregnation process with saturated solution. After heating at 700 °C, a novel needle-shaped NiO is presented, which exhibits some advantages including fast preparation, high connectivity, large specific surface area and high operational stability (i.e. high aggregation resistance). For the purpose of comparison, $Ni(NO_3)_2$ solution impregnated YSZ anodes prepared through the conventional impregnation process are also characterized under the same conditions.



## 1. Introduction

The solid oxide fuel cell (SOFC) is an electrochemical device that converts the energy of a chemical reaction directly into electrical energy [1–3]. It is considered to be a promising candidate of power generation technology in the 21st century due to its many advantages over conventional power-generating systems in terms of efficiency (40–60% unassisted, up to 70% in a pressurized hybrid system), reliability, modularity, fuel flexibility, and environmental friendliness [4,5]. The state-of-the-art material for SOFC anodes is Ni–YSZ (YSZ: Yttria Stabilized Zirconia) cermet that is an excellent catalyst for $H_2$ oxidation [6]. In addition, Ni acts as an electron conductor in the composite. Therefore, contiguous Ni–Ni chains have to be established within the anode to reduce the ohmic resistance and to achieve the percolation threshold, which requires a sufficient amount of Ni be present. However, one of the challenges related to the Ni-based SOFC is the problem of Ni-sintering at high temperatures, leading to Ni particle growth that will result in performance degradation through loss of electrical conductivity of the anode [7]. To the best of our knowledge, there are many researchers focusing on the study of operating stability of the Ni–YSZ anode or the redox stability of the Ni–NiO [8–11]. According to them, the Ni grain growth can take place through different mechanisms: evaporation–condensation, surface diffusion, grain boundary or volume (bulk) diffusion [12–14]. The sintering mechanisms have been found to depend on many process factors, such as, sintering temperature, sintering time, surface energy and interfacial adhesion [15,16]. Some efforts are underway to develop alternative new anode materials for SOFCs to overcome the inevitable Ni sintering [12,17,18]. Despite all this, the Ni–YSZ cermets are still widely used fuel electrodes.

* Corresponding authors. Department of Physics, Harbin Institute of Technology, Heilongjiang 150080, People's Republic of China. Tel./fax: +86 451 86418420.
*E-mail addresses:* zhuxingbao008@163.com (X. Zhu), guanchengzhi@sinap.ac.cn (C. Guan).

0378-7753/$ – see front matter © 2014 Elsevier B.V. All rights reserved.
http://dx.doi.org/10.1016/j.jpowsour.2014.01.058

So far, there are many solutions that have been proposed to improve the operational stability of Ni-based anodes. The first one is to reduce the preparing and operating temperatures in order to avoid the Ni sintering process at elevated temperatures. J.Y. Yoo et al. proposed that Ni–YSZ cermets can be prepared by high frequency induction heated sintering, producing a uniformly porous microstructure without abnormal grain growth found in the conventional sintering method [19]. It is because of this that all sintering processes commence below 1150 °C and finish within 2 min, effectively avoiding the sintering process of Ni at high temperatures. The second one is to optimize the electrode structure (such as functionally graded structure), cermet microstructure (such as grain connectivity, grain size, pore size and pore size distribution), composition and the operating conditions (temperature and humidity) [9,20–23]. Besides temperature, the humidity also boosts Ni growth through increased surface diffusivity of the $Ni_2$–OH complex formed under humid conditions [24]. Finer conductive particles tend to be percolated through the composite material at lower concentrations and lower sintering temperatures, thus resulting in higher freedom in tailoring the Ni–YSZ composition. The third solution proposes to adopt novel but more labor consuming manufacturing techniques like impregnation [25,26]. The purpose of this work at first is to curb the Ni sintering by the introduction of inhibitors, such as, MgO, $Al_2O_3$, $TiO_2$, $CeO_2$, Gd- or Sm-doped $CeO_2$ (GDC or SDC), into the separation of Ni particles. Unfortunately, $TiO_2$ and $Al_2O_3$, and particularly MgO, are indicated to react with Ni and other elements, forming higher resistive phases and decreasing the overall conductivity.

Recently, Ni directly impregnated YSZ anodes were proposed and prepared with expected high catalytic activity owing to its fine particles and long three phase boundary (TPB) [25]. An advantage of the impregnated Ni–YSZ anode is the lower Ni content required to obtain electronic percolation. For this structure, percolation is obtained already around 9 vol% Ni, whereas 30 vol% Ni is required for percolation with the conventional powder based method with 1 μm sized Ni powder [27–29]. Wet impregnation is an alternative and effective technique in the development of the electrode structure which achieves high performance and an advantageous microstructure. However, the disadvantage of wet impregnation is a long preparation time, impregnation cycles >30 and production cycle >1 week [30–32]. Multiple impregnation steps are necessary to achieve sufficient electron conduction (conductive network). Such a repeated impregnation process is time-consuming and hinders the practical application of the impregnation approach [33,34]. Moreover, the repeated cooling and heating cycles are detrimental to the electrolyte membrane, and make it prone to cracking.

So, in this work, we attempt to establish a novel method of fast-preparing $Ni(NO_3)_2$ solution impregnated YSZ anode. The novel anode presents us with a new microstructure resulting in enhanced electrical conductivity and operational stability.

## 2. Experimental

### 2.1. Porous anode-support and cell preparation

Micro-scaled Yttria Stabilized Zirconia powder (YSZ, China) and tapioca (Singapore) were mixed thoroughly at a weight ratio of 5:3, which was then uniaxially pressed into wafers (button cells) with a diameter of 13 mm under a pressure of ~300 MPa, and sintered at 1000 °C for 2 h to guarantee the mechanical strength of green bodies. A dense YSZ electrolyte layer was then attached onto one surface of the pre-sintered wafers through a spin-coating technique and sintered at 1400 °C for 4 h [35]. The Archimedes principle was employed to measure the open porosity of the porous layer after sintering at 1400 °C for 4 h, which is ~60%. A cathode slurry of $La_{0.8}Sr_{0.2}MnO_{3-\delta}$ (LSM) was coated onto the electrolyte membrane surface, and the three-layer was finally co-sintered at 1100 °C for 2 h in air to produce a full cell with a configuration of porous-YSZ|YSZ-membrane|LSM.

### 2.2. Ni impregnated YSZ anode preparation

In this study, there were two different ways to carry out the impregnation process.

#### 2.2.1. The first way ($Way_1$, traditional method)

A $Ni(NO_3)_2$ solution (2 mol·$L^{-1}$) was dipped onto the surface of the YSZ anode support at room temperature, and which was infiltrated into the pores of the porous YSZ layer under capillary action, dried and heated at 300 °C. This impregnation process was repeated until a desired loading (38 wt%) of NiO was achieved.

#### 2.2.2. The second way ($Way_2$, novel method)

Identical YSZ anode supports were soaked in $Ni(NO_3)_2$ saturated solution at a temperature of 80 °C. Here, the cathode was covered and protected with a silver paste (DAD-87, Shanghai Research Institute of Synthetic Resins) that has been solidified at 300 °C. The impregnated pellets were all dried under a home-made vacuum drying device (as shown in Fig. 1) at room temperature. After that, they were all heated at 300 °C. This impregnation process was repeated until a desired loading (38 wt%) of NiO was achieved.

Please note that the concentration of the solution in the first way was controlled to lower than 2 mol $L^{-1}$ in order to avoid the graded distribution of NiO in the thickness direction of the support, which has been demonstrated in our previous work [36]. The impregnated YSZ supports above were all finally fired at 700 °C for 1 h.

### 2.3. Characterization

The specific surface areas of impregnated anodes through different ways were tested using BET method based on an $N_2$ absorption apparatus (JW-BK112, China). The conductivities of different Ni–YSZ anodes were characterized by a four-probe

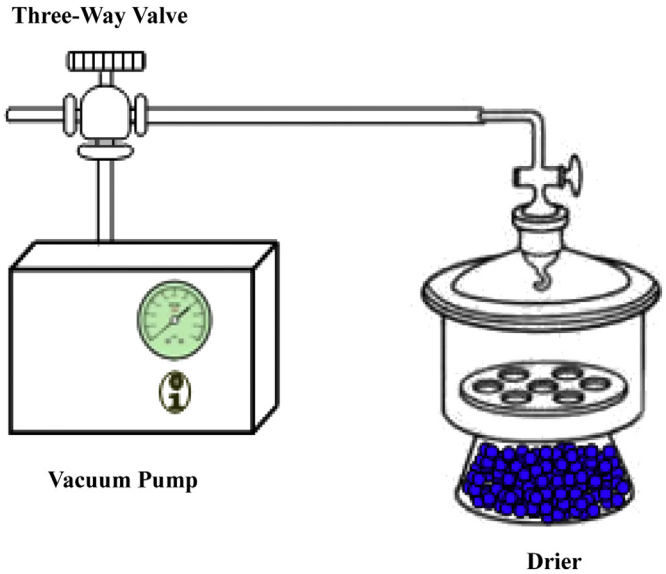


**Fig. 1.** A home-made drying device used for drying impregnated YSZ anode in the second way.

method using a home-made measuring system based on a current source Keithley 2400 and a Keithley 2000 (USA) multimeter. The electrochemical performances of the single cells were measured using a Dual-Channel Potentiostat VSP (Biologic, France). The scanning electron microscope (SEM) images of the anodes were characterized by a FEI Quanta 200F (USA).

## 3. Results and discussion

### 3.1. Microscopy

Fig. 2 shows the SEM images of the two kinds of impregnated anodes. One was prepared using the conventional impregnating process based on a drop-coating technique with low concentration solutions. Increasing concentration seems to be an effective way to reduce impregnation cycles, however it can give rise to an uneven distribution of impregnated particles in porous anode; it has been confirmed in our previous work [36]. The particles will be collected at the support's surface since tiny pores are blocked in previous steps. The tiny pores are considered to be the throat-point or necessary path for solution infiltrating from surface to bottom, which becomes the great limiting factor for the impregnation process and is easily blocked by high concentrated solutions [37]. So, in this study the impregnating solution used in $Way_1$ was controlled to be a low concentration of 2 mol $L^{-1}$. The cross sectional images for the anode (NiO content 38 wt%) prepared via $Way_1$ are shown in Fig. 2(a) and (b), in which many discrete NiO particles with an average grain size of 100 nm evenly distributed over YSZ scaffold. The nano- or micro-particles with high surface energy are prone to agglomerate under preparing and operating conditions, especially for reduction at high temperatures [30,38]. That will cause obvious conductivity loss due to Ni-chain breakage, which is also an important factor for Ni anode instability and performance degradation. Thereby, we proposed a new path to

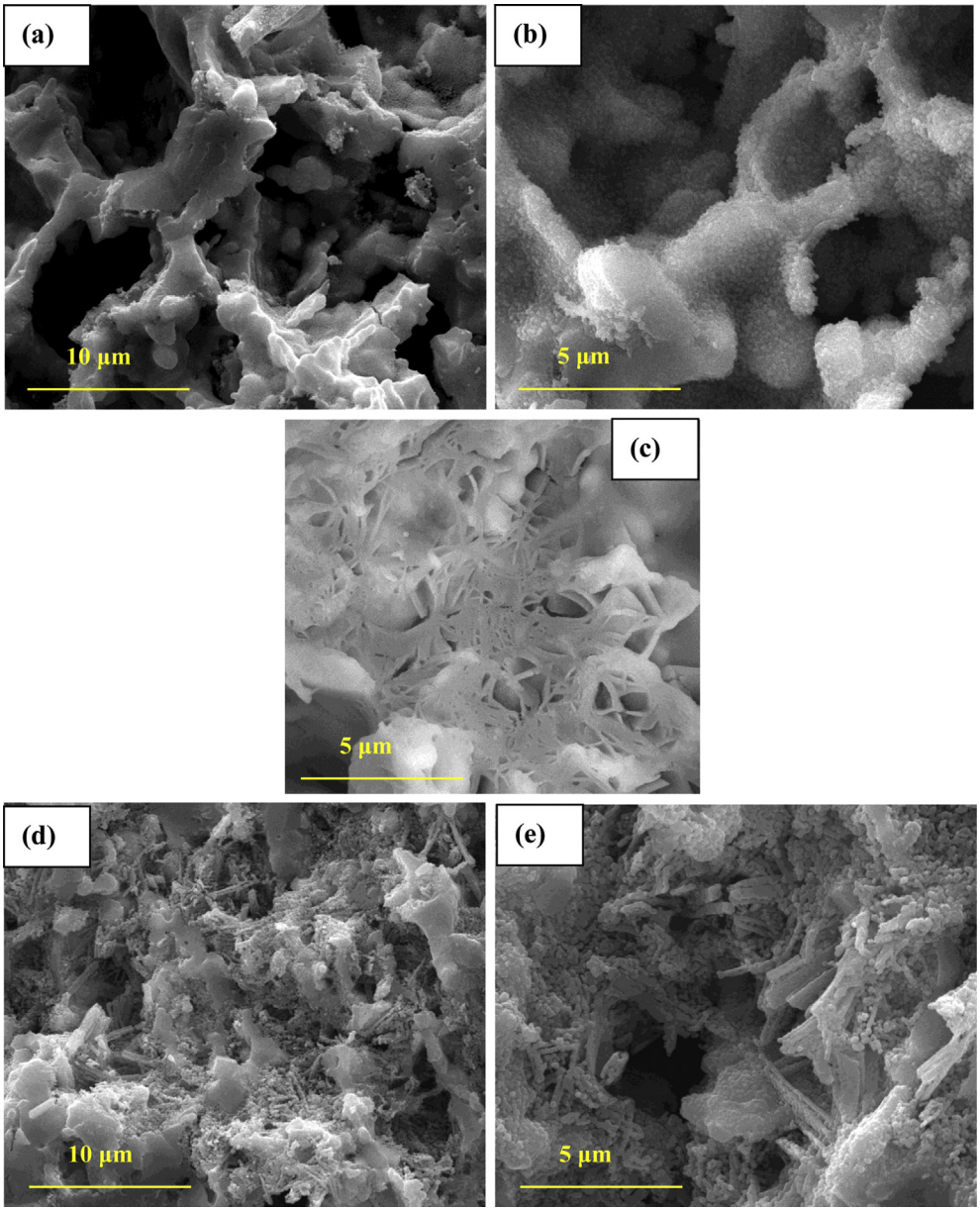


**Fig. 2.** The SEM images for $Ni(NO_3)_2$ solution impregnated YSZ anodes prepared in two different ways. (a), (b) is prepared by $Way_1$ after heated at 700 °C for 1 h, (c) is prepared by $Way_2$ after dried in a home-made device at RT, and (d), (e) is prepared by $Way_2$ after heated at 700 °C for 1 h.

prepare $Ni(NO_3)_2$ solution impregnated YSZ anodes. Here, a saturated solution was directly used to impregnate the porous YSZ support at an increased temperature of 80 °C. The high concentration is aimed to reduce the number of impregnation cycles, while the increased temperature is to aid the impregnation process. The impregnated samples in $Way_2$ were dried in a home-made device as shown in Fig. 1, in which low gas pressure and a desiccant are used to promote fast evaporation at room temperature. Based on the principle of crystallization [39], flower-shaped $Ni(NO_3)_2 \cdot 6H_2O$ crystals are formed inside porous anode support after the drying process, as shown in Fig. 2(c) and the structure is still kept after thermolysis and sintered at high temperatures, as shown in Fig. 2(d) and (e), resulting in needle-shaped NiO and thus Ni. The re-crystallization during the drying process in $Way_2$ (but not $Way_1$) causes the redistribution of $Ni(NO_3)_2 \cdot 6H_2O$ crystals, forming a more porous structure with many fractures in Fig. 2(c) which is favorable for the impregnation process. This is also the major reason why the saturated solution can be directly used for impregnation in $Way_2$. Of course, a higher temperature of 80 °C is necessary as well. As shown in Fig. 2(d) and (e), the resulting needle-shaped NiO is quite easy to connect to each other, achieving expected high conductivity. Moreover, this microstructure has the advantages of resisting NiO or Ni aggregation due to the pre-condensation during the redistribution/drying process, indicating an expected high operational stability. Compared to (a) and (b), the NiO particles in (d) and (e) are more porous, which can make good use of the three dimensional space in pores by forming needle-shaped NiO. According to cavity model [36], the porosity of a porous YSZ support (with original porosity of 60%) will be decreased to 49% after the impregnation of 38 wt% NiO using $Way_1$ (with an average grain NiO size of 100 nm), indicating the space in a porous anode is not used effectively. But further improving the NiO content using $Way_1$ will cause more tiny pores to block, resulting in grade distribution of NiO, and lead to electrochemical performance loss due to dense NiO layers formed over the YSZ scaffold which will hinder the gas flow to TPB and then suppress the anode reaction [3,30,40].

### 3.2. Preparation efficiency and conductivity measurements

Fig. 3 shows the dependence of the loading on the times of impregnating–heating cycles in the two kinds of anodes. The change of the loading with the cycle times can be estimated from a simple model (cavity model) [36]. The cavity was used to simulate a pore in the porous YSZ anode support. It can be seen from Fig. 3 that the preparation efficiency of $Way_2$ is 3 times higher than that of $Way_1$, which would be advantageous in keeping the mechanical strength of impregnated anodes as well as SOFCs. Also it has an important significance in the promotion of impregnating techniques.

The conductivity curves of the $Ni(NO_3)_2$ solution impregnated YSZ anodes prepared in two different ways were tested with the four probe method, and the results are shown in Fig. 4. Before testing, the two kinds of anodes were all reduced under pure $H_2$ condition at 700 °C for 1 h, and the data was recorded from 700 °C to 200 °C with a cooling rate of 10 °C $min^{-1}$. It can be seen that the electrical conductivities for the two kinds of anodes all decrease with the increasing temperature, indicating electron conduction is dominant, and confirming an Ni-network has been formed in the two impregnated anodes. At 700 °C, the lowest conductivity for the anode prepared via $Way_2$ is 369 S $cm^{-1}$, which is high enough for SOFC electrochemical reaction. It is also 7 times the conductivity of the anode prepared via $Way_1$, demonstrating a more reliable and effective connective-network has been constructed in the needle-shaped Ni anode. The reason for low conductivity of the anode prepared via $Way_1$ may be due to the coarsening of Ni particles at the elevated temperatures and the loss of Ni particle connectivity. Particle coarsening and surface diffusion are less likely to occur in the needle-shaped Ni anode since the fine particles have been coarsened and closely connected with each other to form needle during the re-distribution/drying process.

### 3.3. Specific surface area measurements

It is well known that in SOFC systems the electrodes provide the sites for electrochemical reactions [31,41]. In fact the site is the specific surface area including adsorption area and TPB. TPB is the most active area in electrodes where the electron, ion and gas meet. The adsorption area has a good ability to adsorb reaction gas to start and push the electrochemical reaction process forward. One important method to enhance the activity of SOFC electrodes is to expand TPB and adsorption area, i.e. specific surface area [32,42]. So, the adsorption areas of two kinds of impregnated anodes with the same NiO content were tested through BET method. As shown in Fig. 5, the adsorption area of the anode impregnated with $Way_2$ is 7.48 $m^2$ $g^{-1}$, which is 1.14 times larger than that of the anode impregnated with $Way_1$, demonstrating a more porous microstructure for the needle-shaped NiO in Fig. 2(d) and (e), with an expanded surface area and an enhanced performance.

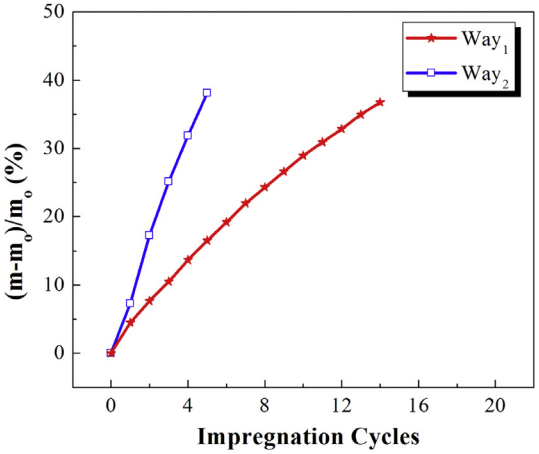


**Fig. 3.** Dependence of NiO loadings on cycle times in the two different ways.

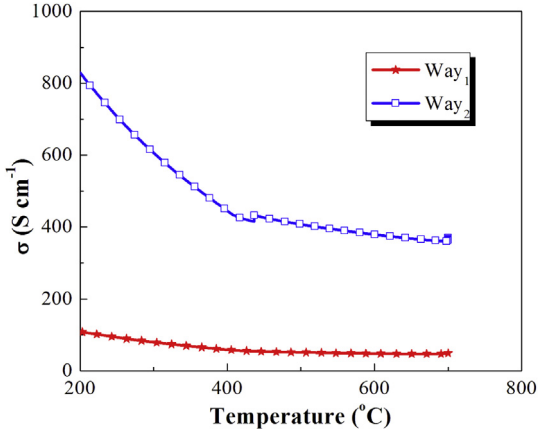


**Fig. 4.** The conductivities of $Ni(NO_3)_2$ solution impregnated YSZ anodes prepared by two different ways.

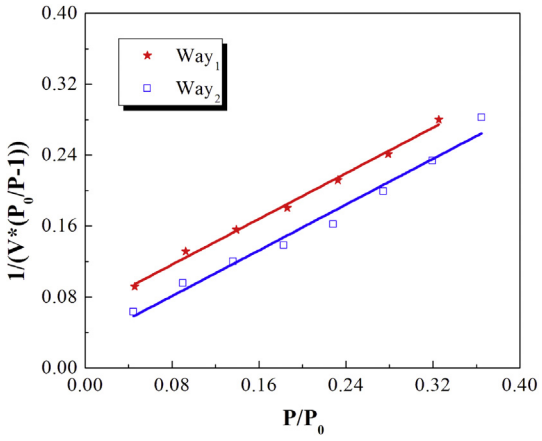


**Fig. 5.** Adsorption curves of $Ni(NO_3)_2$ solution impregnated YSZ anodes prepared in two ways.

### 3.4. Characterization of the electrochemical performance of single cells

The VSP Multichannel Potentiate was used to characterize the electrochemical performances of single SOFCs with a configuration of NiO–YSZ|YSZ|LSM. Two cells were named as Cell-1 and Cell-2, with anodes prepared via $Way_1$ and $Way_2$, respectively. Fig. 6 compares the cell voltage change of Cell-1 with time under a constant current density of 400 mA $cm^{-2}$ at 700 °C. Clearly, some degradation was observed for Cell-1, as the cell voltage dropped from 0.77 V to 0.72 V. The degradation rate was 6.2% over 14 h (~0.44% per hour). For Cell-2, the cell voltage decreased from 0.83 V to 0.82 V (1.1% decrease over 16 h, ~0.06% per hour). More importantly, after operation for 16 h, the performance of Cell-2 became steady, but not for Cell-1. In the last 5 h, the degradation rate for Cell-2 was close to 0%; in contrast the degradation rate for Cell-1 was still ~0.23% per hour. For the conventional Ni–YSZ anode, the degradation rate is no less than 0.3% per hour, especially in the starting period [2,3,43]. The potential drop could be ascribed to a slight reduction of the effective TPB due to rearrangement or coalescence of Ni nanoparticles. Sintering of Ni is a key stability issue for Ni–YSZ anodes, and especially infiltration based electrodes. Fortunately the deterioration of electrode performance can be basically inhibited by using the proposed impregnation method. In the anode prepared by the novel method, NiO or Ni presents a structural characteristic of needle but not nano-particles, and therefore sintering of Ni particles are somewhat retarded.

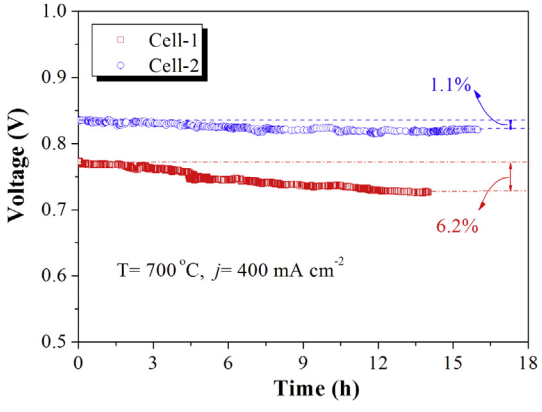


**Fig. 6.** Stability tests for single cells with $Ni(NO_3)_2$ solution impregnated YSZ anodes prepared in two different ways.

## 4. Conclusions

In this study, an improved impregnation process is used to prepare a novel needle-shaped NiO into porous YSZ matrix. Compared to the conventional impregnation process, the new method improves preparation efficiency by 3 times, which is expected to be a tremendous force for the large scale application of the impregnation technique. This novel impregnated anode exhibits a large specific surface area of 7.48 $m^2 g^{-1}$, which is 1.14 times larger than that of anode impregnated through the conventional process. Moreover the electrical conductivity of the novel anode is 369 S $cm^{-1}$ at 700 °C, which is 7 times higher than that of the conventional impregnated anode. The operational stabilities for single cells with the two kinds of anodes are also compared. The degradation rate for the cell with the novel anode is 1.1% over 16 h tests, while the degradation rate for the cell with the conventional impregnated anode is 6.2% over 14 h. The former cell's performance becomes steady after operation for 6 h, but not for the latter one with ~1% degradation over the last 5 h.

## Acknowledgments

This work was supported by Foundation of Harbin Institute of Technology (HIT.NSRIF.2013088), Natural Science Foundation of China (21206023), the Postdoctoral Fund (LBH-Z12088 and 2013M531031) and Hong Kong Scholars Program (XJ2013014).

## References

[1] D. Sarantaridis, A. Atkinson, Fuel Cells 7 (2007) 246–258.
[2] W.Z. Zhu, S.C. Deevi, Mater. Sci. Eng. A 362 (2003) 228–239.
[3] S.P. Jiang, Mater. Sci. Eng. A 418 (2006) 199–210.
[4] S. Park, J.M. Vohs, R.J. Gorte, Nature 404 (2000) 265–267.
[5] S.W. Tao, J.T.S. Irvine, Nat. Mater. 2 (2003) 320–323.
[6] B.C.H. Steele, A. Heinzel, Nature 414 (2001) 345–352.
[7] A. Atkinson, S. Barnett, R.J. Gorte, J.T.S. Irvine, A.J. McEvoy, M. Mogensen, S.C. Singhal, J. Vohs, Nat. Mater. 3 (2004) 17–27.
[8] S. Vogel, E. Ustundag, J.C. Hanan, V.W. Yuan, M.A.M. Bourke, Mater. Sci. Eng. A 333 (2002) 1–9.
[9] M.H. Pihlatie, A. Kaiser, M.B. Mogensen, Solid State Ionics 222 (2012) 38–46.
[10] B. Liu, Y. Zhang, B.F. Tu, Y.L. Dong, M.J. Cheng, J. Power Sources 165 (2007) 114–119.
[11] K. Sato, H. Abe, T. Misono, K. Murata, T. Fukui, M. Naito, Fuel Cells Bull. 2009 (2009) 12–16.
[12] S.P. Jiang, S.H. Chan, J. Mater. Sci. 39 (2004) 4405–4439.
[13] T. Talebi, M.H. Sarrafi, M. Haji, B. Raissi, A. Maghsoudipour, Int. J. Hydrogen Energy 35 (2010) 9440–9447.
[14] A. Buyukaksoy, V. Petrovsky, F. Dogan, J. Electrochem. Soc. 159 (2012) B666–B669.
[15] M. Pihlatie, A. Kaiser, M. Mogensen, Solid State Ionics 180 (2009) 1100–1112.
[16] X.C. Song, J. Lu, T.S. Zhang, J. Ma, J. Eur. Ceram. Soc. 31 (2011) 2621–2627.
[17] X.B. Zhu, Z. Lü, B. Wei, K.F. Chen, M.L. Liu, X.Q. Huang, W.H. Su, J. Power Sources 190 (2009) 326–330.
[18] E.V. Tsipis, V.V. Kharton, J. Solid State Electrochem 12 (2008) 1367–1391.
[19] J.Y. Yoo, C.K. Cho, I.J. Shon, K.T. Lee, Mater. Lett. 65 (2011) 2066–2069.
[20] M. Marinšek, K. Zupan, Ceram. Int. 36 (2010) 1075–1082.
[21] D. Waldbillig, A. Wood, D.G. Ivey, J. Electrochem. Soc. 154 (2007) B133–B138.
[22] M. Pihlatie, T. Ramos, A. Kaiser, J. Power Sources 193 (2009) 322–330.
[23] Y.H. Koh, J.J. Sun, H.E. Kim, Mater. Lett. 61 (2007) 1283–1287.
[24] J. Sehested, J.A.P. Gelten, I.N. Remediakis, H. Bengaard, J.K. Nørskov, J. Catal. 223 (2004) 432–443.
[25] T. Klemensø, K. Thydén, M. Chen, H.J. Wang, J. Power Sources 195 (2010) 7295–7301.
[26] T. Fukui, S. Ohara, M. Naito, K. Nogi, J. Power Sources 110 (2002) 91–95.
[27] S.F. Corbin, X. Qiao, J. Am. Ceram. Soc. 86 (2003) 401–406.
[28] F.H. Wang, R.S. Guo, Q.T. Wei, Y. Zhou, H.L. Li, S.L. Li, Mater. Lett. 58 (2004) 3079–3083.
[29] D. Simwonis, F. Tietz, D. Stöver, Solid State Ionics 132 (2000) 241–251.
[30] S.P. Jiang, Int. J. Hydrogen Energy 37 (2012) 449–470.
[31] P.R. Shearing, D.J.L. Brett, N.P. Brandon, Int. Mater. Rev. 55 (2010) 347–363.
[32] Z.Y. Jiang, C.R. Xia, F.L. Chen, Electrochim. Acta 55 (2010) 3595–3605.
[33] R.J. Gorte, J.M. Vohs, Annu. Rev. Chem. Biomol. Eng. 2 (2011) 9–30.

[34] M.L. Liu, M.E. Lynch, K. Blinn, F.M. Alamgir, Y.M. Choi, Mater. Today 14 (2011) 534–546.
[35] X.B. Zhu, Z. Lü, B. Wei, K.F. Chen, M.L. Liu, X.Q. Huang, W.H. Su, J. Power Sources 195 (2010) 1793–1798.
[36] X.B. Zhu, Z. Lü, B. Wei, M.L. Liu, X.Q. Huang, W.H. Su, Electrochim. Acta 55 (2010) 3932–3938.
[37] W. Zhu, D. Ding, C.R. Xia, Electrochem. Solid-State Lett. 11 (2008) B83–B86.
[38] L.P. Li, P.G. Zhang, R.R. Liu, S.M. Guo, J. Power Sources 196 (2011) 1242–1247.
[39] M. Chauhan, F.A. Mohamed, Mater. Sci. Eng. A 427 (2006) 7–15.
[40] B. Zhu, Int. J. Energy Res. 33 (2009) 1126–1137.
[41] R.J. Gorte, J.M. Vohs, Curr. Opin. Colloid Interface Sci. 14 (2009) 236–244.
[42] J.S. Qiao, K.N. Sun, N.Q. Zhang, B. Sun, J.R. Kong, D.R. Zhou, J. Power Sources 169 (2007) 253–258.
[43] T. Matsui, R. Kishida, J.Y. Kim, H. Muroyama, K. Eguchi, J. Electrochem. Soc. 157 (2010) B776–B781.